energies

MDPI

Article

Exergetic and Economic Improvement for a Steam Methane-Reforming Industrial Plant: Simulation Tool

Francisco Jose Durán, Fernando Dorado and Luz Sanchez-Silva *

Department of Chemical Engineering, University of Castilla—La Mancha, Avda. Camilo José Cela 12, 13071 Ciudad Real, Spain; fran.duran.1995@hotmail.com (F.J.D.); fernando.dorado@uclm.es (F.D.)
* Correspondence: marialuz.sanchez@uclm.es; Tel.: +34-926295300 (ext. 6307); Fax: +34-926295256

Received: 16 June 2020; Accepted: 20 July 2020; Published: 24 July 2020

Abstract: Steam methane reforming (SMR) for hydrogen production was studied by simulating the reformer and pre-reformer sections. This simulation was validated by using available data taken from a real industrial plant, which enabled precise correlations with the real industrial process to be found. Moreover, the influence of the molar ratio between the raw materials (steam-to-carbon molar ratio, S/C) and the reformer outlet temperature (T_{cc}) was studied. The energy requirements for the reforming reaction increased with the S/C ratio. The energy needed for developing the reforming reaction also increased with T_{cc}, but the hydrogen yield when operating with a high S/C ratio and T_{cc} increased. In addition, an exergetic analysis was carried out to identify exergy losses in the SMR process, and most were destroyed in the chemical reactors. Increasing the combustion air flow was proposed for finding an optimum value for exergetic efficiency in the process, thereby reducing fuel consumption. Finally, there was a study into the economic viability of this investment, with a reduction of 22% in utility costs with the optimum exergetic value.

Keywords: steam methane reforming; simulation software; hydrogen yield; industrial plant; exergetic analysis; economic study

1. Introduction

Between 2000 and 2013, global energy demand grew by 38%. It is estimated that the world population will reach approximately 7.5 billion in 2025, with a 50–60% increase in global energy consumption in relation to current consumption [1]. Recently, many leading energy, transport and industrial companies have started initiatives to develop the energy transition with hydrogen [2]. However, to satisfy the increasingly demand for it, large-scale industrial processes must be developed for producing it. One such process is partial oxidation [3], in which a hydrocarbon feedstock is partially oxidized with oxygen to produce hydrogen after an exothermal reaction. Another method used is hydrocarbon pyrolysis, in which hydrogen is obtained after the thermal decomposition of a hydrocarbon feedstock. However, one of the best methods for large-scale hydrogen production is steam methane reforming (SMR). SMR is an endothermal process in which methane reacts with steam to produce hydrogen. In this process, high-purity hydrogen can be obtained and different by-products generated during the reforming reactions can be reused. Over 50% of the world's H_2 production comes from SMR [4].

Therefore, large amounts of energy are required in these industrial processes, and it is essential to know the maximum amount of energy they need. To better understand this, many authors have carried out different energetic analyses in which key variables were studied to identify how to make the industrial plant, as a whole, more energy efficient. Process simulation software was used in this research as an optimal tool for modelling these chemical processes. In this respect, Imran et al. [5] developed a simulation, validation and sensitivity analysis of typical SMR using Aspen Plus® software.

They concluded that the steam-to-carbon ratio and reformer temperature were two of the most important variables for optimizing the process. Similarly, Pashchenko [6] studied heat integration in the reformer section. A schematic diagram was made of thermochemical recovery by steam methane reforming. Moreover, Cui et al. [7] simulated cracking, partial oxidation, steam reforming and oxidative steam reforming of butane and propane in order to predict carbon formation and catalysts deactivation, using Gibbs free energy minimization method in Aspen Plus®. They found that carbon formation only occurred at low steam-to-carbon ratios, while the maximum level of carbon formation was found at 550–650 °C.

With the data obtained from the software simulation, modifications in the process that may potentially improve energetic performance may be studied. Energy efficiency is evaluated as being the ratio of the amount of energy that enters and leaves a system and is obtained by energy balances. Even though this kind of analysis is quite useful for optimizing the process, it can neither identify efficiencies nor evaluate them correctly. For this reason, the second law of thermodynamics and the exergy concept are applied. The exergy of a thermodynamic system may be defined as the quantity of useful work that this system could do when it is brought into equilibrium with its surroundings.

Many authors have already developed this kind of analysis in different chemical processes. BoroumandJazi et al. [8] used the exergetic analysis for studying different industrial sectors in a variety of countries. They evaluated the performance of the industry and linked this analysis with CO_2 emissions and life-cycle assessment studies. They found that there were significative differences between energy and exergy efficiency and stressed that the second law of thermodynamics was crucial for optimizing energy efficiency. Furthermore, Kaini and Mondal [9] compared different hydrogen production methods such as steam methane reforming. They applied this analysis in order to identify where most exergy is lost. Most destruction of exergy is due to the high irreversibility of chemical reactions.

In particular, some authors also performed this kind of analysis in steam methane reforming. Martínez-Valiente et al. [10] developed a kinetic, energetic and exergetic approach to tri-reform methane. They found that the chemical reactors in the process were the units in which most exergy was destroyed. This study confirms that the exergy destruction is caused by the high irreversibility of chemical reactions.

A similar exergetic analysis has been carried out for hydrogen production via dry gas reforming. Dry gas reforming was simulated, and the exergetic efficiency was calculated, showing an efficiency of 55%. [11]. Behroozsarand et al. [12] studied different methods for hydrogen production, with the autothermal reforming one being one of the most efficient methods from the exergetic point of view.

There are several works that recommend optimal operative conditions for different reforming processes. Zouhour Khila et al. [13] performed environmental life-cycle assessment analyses as a tool for optimization of hydrogen production by autothermal reforming. They recommend the operation with a feed molar ratio of 4 and a reforming temperature of 800 °C.

In this paper, there was a computer-aided simulation of steam methane reforming to produce hydrogen with the Aspen HYSYS® software. This simulation was developed to evaluate where the exergetic losses are located in order to improve the energetic performance of the process. The analysis presented herein used an equilibrium model for making the chemical reactions (reformer and shift reactions) in this study. In addition, the data available from the industrial plant at the Puertollano petrochemical refinery (Spain) helped to validate the simulation and meant it was extremely reliable in terms of representing real outcomes. This plant provides hydrogen to the petrochemical refinery, also located in Puertollano, with a production capacity of up to 47.500 Nm^3/h, which satisfies the demand of the refinery for sulphur-free fuels. Note that, contrary to most works on this topic, the simulation data are not based on general estimations for this process but, rather, on empirical data taken from the plant. Hence, the calculations made by the simulation accurately reproduce how the plant responds to changes in operational variables.

In addition, an energetic analysis of the simulation process could provide an insight as to what the optimal values are for some key variables [5–10]. In this respect, a sensitivity and optimization analysis

of the most important variables—the steam-to-carbon molar ratio and the reformer temperature—were performed. Furthermore, there was an exergetic analysis of the steam methane reforming plant in order to assess precise losses in exergy, and this allowed alternatives for increasing exergy efficiency to be proposed. Finally, there was a preliminary economic analysis of any exergetic improvements.

2. Methodology

2.1. Model Description

The simulation is composed of two different sections: reformer and pre-reformer (Section 1, Figure 1a) and the shift section (Section 2, Figure 1b).

In order to develop the simulation of both sections, the conditions of each stream and block involved must be known, and these were extracted from the simplified process flow diagram of the plant and are shown in Tables 1–4. In addition, the following assumptions were made [4,10]:

(1) Steady state and isothermal process.
(2) Catalyst deactivation and coke formation were not considered. If catalyst deactivation is considered, the performance of chemical reactors would have been worse, so the exergetic efficiency should decrease as well.
(3) No heat losses took place in the pre-reformer (P-REF), reformer furnace (REF-F) and reformer tubes (REF).
(4) Pressure losses in heat exchangers pre-heater 1 (P-HEAT 1) and pre-heater 2 (P-HEAT 2) were 320 kPa and 150 kPa, respectively.
(5) The outlet pressures of each mixing unit (called MIX) were considered equal to the lowest one of the inlet streams.
(6) All gases were ideal.
(7) Sulphur was not considered in the fuel inlet stream.
(8) No pressure losses were considered except in the shift reactor (100 kPa).
(9) The stream named "null" had no molar flow.
(10) Pure water was considered on the cool side of the heat exchangers in Section 2. The temperature of these streams was adjusted to the simplified process flow diagram (PFD) of the steam methane-reforming plant at the Puertollano petrochemical refinery.

Table 1. Inlet stream conditions in Section 1.

Stream	Pressure (bar)	Temperature (°C)
SYN-GAS HDS	35.2	345
STEAM	44.4	322
AIR	0.1	32
FUEL	0.1	345

Table 2. Description of the blocks used in Section 1.

Name	Type	Description
P-REF	Equilibrium reactor	It was used to perform the pre-reforming reactions, converting heavier hydrocarbons into methane and hydrogen.
REF	Equilibrium reactor	It was used to develop the reforming reactions, in which almost all methane was converted into hydrogen and carbon monoxide.
REF-F	Equilibrium reactor	This block was used for estimating the amount of fuel required. This unit depends on the energy consumption in the REF unit.
MIX-1	Mixer	This unit was used for adjusting the ratio between the raw materials.
MIX-2	Mixer	In this block, the fuel was mixed with the off-gas stream.
P-HEAT 1	Heat Exchanger	The unit in which raw materials introduced were first heated before the pre-reforming reactions

Table 2. *Cont.*

Name	Type	Description
P-HEAT 2	Heat Exchanger	The unit in which raw materials introduced were first heated before the reforming reactions
SOP-1	Compressor	This block was used to compress the air necessary for combustion reactions.
PRE-COLD AIR	Cooler	In this block, the air was cooled after being sent into the furnace.

Table 3. Feed stream conditions in Section 2.

Stream	Pressure (bar)	Temperature (°C)	Composition (mol %)
Feed from Section 1	30.5	920	H_2—54; N_2—1.4; CO—13.8; CO_2—3.9; CH_4—5.43; H_2O—21.1
BFW IN 1	43.1	256	H_2O—100
BFW IN 4	43.1	111	H_2O—100
BFW IN 5	43.1	109	H_2O—100

Table 4. Description of the blocks used in Section 2.

Name	Type	Description
SHIFT	Equilibrium reactor	It was used for performing the shift reaction, converting carbon monoxide into carbon dioxide.
CONDENSATES SEPARATOR	Separator	In this block, all the water present in the shift outlet stream was removed.
HYDROGEN SEP	Splitter	This unit was used for adjusting hydrogen recovery after the shift outlet stream was purified.
PRECOLD-1	Heat Exchanger	In this unit, the high temperature reformer stream was cooled.
PRECOLD-2	Heat Exchanger	This block adjusted the inlet temperature of the shift reactor.
PRECOLD-3	Heat Exchanger	This block adjusted the outlet temperature of the shift reactor.
PRECOLD-4	Heat Exchanger	In this unit, the outlet stream of the shift reactor was cooled before water separation in the CONDENSATES SEPARATOR unit.
PRECOLD-5	Heat Exchanger	In this unit, the outlet stream of the shift reactor was cooled before water separation in the CONDENSATES SEPARATOR unit.
SEP-1	Tee	This block adjusted the syn-gas flow through PRECOLD-2.
SEP-2	Tee	This block adjusted the syn-gas flow through PRECOLD-3.
SEP-3	Tee	This block adjusted the coolant flow through PRECOLD-5.
SEP-4	Tee	This block adjusted the coolant flow through PRECOLD-2 and PRECOLD-4.
MIX-3	Mixer	In this unit, the shift inlet temperature was adjusted.
MIX-4	Mixer	In this unit, the shift outlet temperature was adjusted.
MIX-5	Mixer	This block recovered the coolant used in PRECOLD-5 and sent it to SEP-4.

Firstly, the components needed in the feed stream (natural gas, NG) were specified. NG was provided by the national network and so could vary in its makeup, and its proximate composition is shown in Table S1 (data obtained from NG analytics). NG was used as a fuel in the reformer furnace. In order to simulate the reformer section, the conditions of the inlet stream at this stage were obtained from the industrial plant data, for which the composition was reported in the simplified process diagram of the industrial plant and is shown in Table S2.

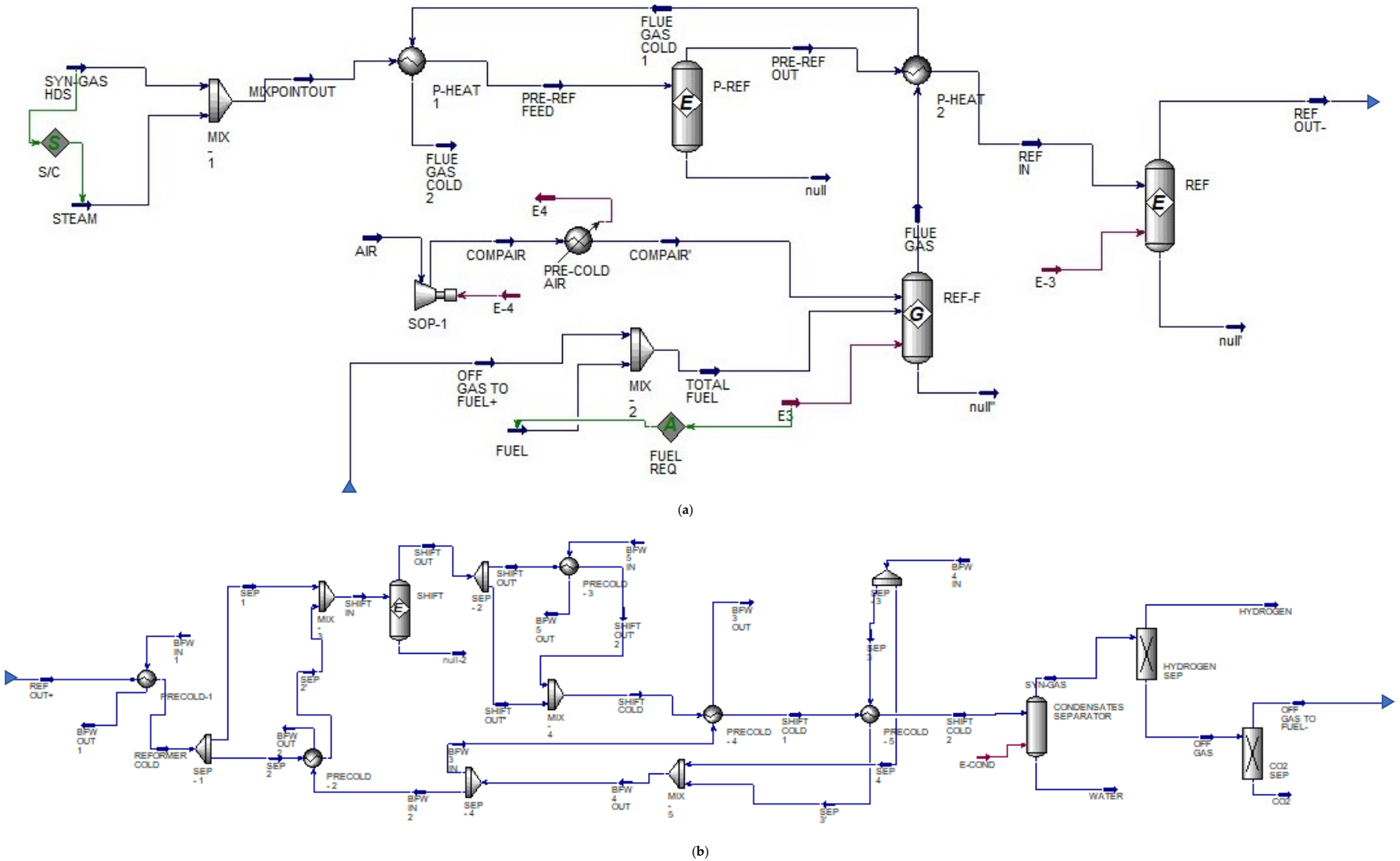

Figure 1. (**a**) Section 1—reformer section Aspen HYSYS® process flow diagram; (**b**) Section 2—shift section Aspen HYSYS® process flow diagram.

2.1.1. Section 1—Reformer Section

Once the natural gas was sulphur-free, it was sent to the reformer section, where the hydrocarbons present in the natural gas reacted with steam to produce hydrogen and carbon monoxide, as in Equation (1). In this unit, most of the total hydrogen is produced. If the energetic performance of this reactor is enhanced, the whole process would improve.

$$CH_4 + H_2O \leftrightarrow CO + 3H_2 - \text{Heat} \quad (1)$$

This reaction took place in the reformer reactor (REF) and was so endothermal that temperatures of up to 1000 °C were required in the furnace. For this reason, an energy analysis of this section of the process was necessary. The Aspen HYSYS® process flow diagram is shown in Figure 1a. In this case, the reforming reactor studied consists of a tubular side-fired reformer. The feed is introduced on the top of the reactor to adjust the ratio between natural gas and steam at the inlet of this reactor (S/C ratio). Adjusting this ratio allows to perform optimization of the reforming reactor. If a low S/C ratio is used, the energy consumed in the reforming reaction would be low, but less hydrogen would be produced as well.

To obtain the highest amount of hydrogen in the reforming reaction, a pre-reforming reactor (P-REF) was located upstream. The pre-reforming reactor was also studied to simulate each of the chemical reactors involved in the process. In this reactor, the heaviest hydrocarbons in natural gas are reformed into smaller molecules, during which a small amount of hydrogen is produced. In this case, the pre-reforming reactions considered are Equations (1)–(4).

$$C_2H_6 \text{ Steam reforming}: \ C_2H_6 + H_2O \rightleftharpoons CO + CH_4 + 2H_2 \qquad \Delta H_{298} = 140 \text{ kJ/mol} \quad (2)$$

$$C_3H_8 \text{ Steam reforming}: \ C_3H_8 + H_2O \rightleftharpoons CO + 2CH_4 + H_2 \qquad \Delta H_{298} = 85 \text{ kJ/mol} \quad (3)$$

$$\text{Water gas shift}: \ CO + H_2O \leftrightharpoons CO_2 + H_2 \qquad \Delta H_{298} = 41 \text{ kJ/mol} \quad (4)$$

2.1.2. Section 2—Shift Section

The reforming reaction also gave off CO as a by-product, which must be removed from the hydrogen before sending it to the customer. Therefore, it is oxidized to CO_2 in the shift reactor, where Equation (4) takes place. The process flow diagram of this section is shown in Figure 1b which involved the shift reactor and the syn-gas cooling section.

The shift reaction is exothermal, so the heat generated during the reaction must be thoroughly removed. It is carried out through a cooling train which is composed of different heat exchangers that remove the heat of this stream. This heat is used to preheat boiling feed water that is fed into a boiler. The boiler and the rest of the steam generation unit was not considered in this simulation.

The outlet stream of this reactor is mainly composed of hydrogen and carbon dioxide. The latter is removed from the hydrogen by means of an amine-based absorption and a flash tower. In this section of the process, the carbon dioxide can be separated from the hydrogen which is purified downstream.

2.2. Exergetic Analysis

Exergy balances are the combination of energy and entropy balances. The exergy of a system could be defined as the maximum work that can be obtained from a system during a process that brings it into thermodynamic equilibrium with its surroundings, with a reference state characterized by a temperature T_0 and a pressure P_0. [10] In this sense, exergetic analysis provides a more precise analysis of the energetic performance in the considered industrial process.

Any irreversible phenomena can cause exergy losses. In this regard, the objective of this kind of analysis is to find these irreversible phenomena in the process under observation. Some of the most remarkable characteristics of exergy are listed below [8]:

- A system in complete equilibrium with the environment has zero exergy, and the more it deviates from its surroundings, the more exergy it has.
- When one type of energy is transformed into another, the result is a loss of exergy.
- As the exergy depends on the environment, a standard environment with a given chemical composition, temperature and pressure must be defined.
- Studying exergy allows a design engineer to aim for the highest possible technical efficiency at a minimum cost. This kind of analysis provides an insight as to where losses and possible improvements can be determined.

There are three ways of transferring exergy: heat interaction, work interaction or mass flow. Kinetic and potential components of exergy were not considered in this study. The mathematical equations have been extracted from different research [7,10,14]. Some of the equations applied in these papers have not been considered in this analysis. Thus, for purposes of simplifying the mathematical calculations, the equation for unused exergy has not been taken into account.

Exergy associated with heat interaction could be calculated by using Equation (5). Thermal flow exergy, Ex_Q, is the maximum amount of work that could be developed for the same heat stream at a given temperature.

$$Ex_Q = Q \cdot \left(1 - \frac{T_0}{T}\right) \tag{5}$$

where Q is the amount of heat in the stream, kJ/h; T_0 is the reference temperature of the environment, K; and T is the heat transmission temperature, K.

The exergy associated with workflow, Ex_w, corresponds with the total workflow in the process. This exergy was proportional to all of the work involved in the process, W.

$$Ex_W = W \tag{6}$$

Mass flow exergy is the sum of chemical exergy (Ex_{CHEM}); physical exergy, Ex_{PHYS}; and mixture exergy, Ex_{MIX} (Equation (7)).

$$Ex_M = Ex_{PHYS} + Ex_{CHEM} + Ex_{MIX} \tag{7}$$

Each of the previous terms could be calculated with different equations. Physical exergy is the amount of work that could be obtained from the substance in a physical reversible process, and this could be calculated through Equation (8).

$$Ex_{PHYS} = [(H - H_0) - T_0 \times (S - S_0)] \cdot n \tag{8}$$

where Ex_{PHYS} is the physical exergy of the material stream, kJ/h; n is the molar flow of the stream, kmol/h; H is the molar enthalpy of the stream, kJ/kmol; H_0 is the molar enthalpy of the stream in reference state, kJ/kmol [15]; T_0 is the reference state temperature, K; S is the molar entropy of the stream, kJ/kmol·K; and S_0 is the molar entropy of the stream in reference state, kJ/kmol·K [16].

Chemical exergy is the amount of work that could be extracted from a substance if a thermodynamic equilibrium state is reached through chemical reactions. This term could be evaluated by using Equation (9).

$$Ex_{CHEM} = n \cdot \left(L_0 \cdot \sum_{i=1}^{n} X_{i,0} \cdot Ex^{0L}_{CHEM,i} + V_0 \cdot \sum_{i=1}^{n} Y_{i,0} \cdot Ex^{0v}_{CHEM,i} \right) \tag{9}$$

where Ex_{CHEM} is the chemical exergy of the stream, kJ/h; n is the molar flow of the stream, kmol/h; L_0 is the liquid fraction of the stream in the reference state; $X_{i,0}$ is the liquid fraction in the reference state of each component; $Ex^{0L}{}_{CHEM,i}$ is the standard chemical exergy in the reference state (liquid phase), kJ/kmol [10]; V_0 is the vapour fraction in the reference state; $Y_{i,0}$ is the vapour fraction in the reference state of each component; and $Ex^{0v}{}_{CHEM,i}$ is the standard chemical exergy in the reference state (vapour phase), kJ/kmol [10].

Finally, mixture exergy could be calculated through Equation (10).

$$\Delta Ex_{MIX} = (\Delta H_{MIX} - T_0 \cdot \Delta S_{MIX}) \cdot n \quad (10)$$

For ideal gas, ΔH_{MIX} is equal to zero. ΔS_{MIX} should be calculated by using Equation (11).

$$\Delta S_{MIX} = \Delta S - \sum_{i=1}^{n} x_i \cdot \Delta s_i = (S - S_0) - \sum_{i=1}^{n} x_i \cdot (S_i - S_{i,0}) \quad (11)$$

where ΔEx_{MIX} is the mixture exergy in the stream, kJ/h; ΔH_{MIX} is the increase in enthalpy in the mixture, kJ/kmol; T_0 is the reference state temperature, K; ΔS_{MIX} is the increase in entropy in the mixture, kJ/kmol·K; n is the molar flow of the stream, kmol/h; S is the entropy of the stream, kJ/mol·K; S_0 is the entropy of the stream in standard conditions, kJ/kmol·K [16]; x_i is the molar fraction of each component; S_i is the molar entropy of each component of the stream, kJ/kmol·K; and $S_{i,0}$ is the molar entropy of each component of the stream in standard conditions, kJ/kmol·K.

Once each exergy term was calculated for each block, exergy efficiency could be calculated. With Equation (12), we could find the exergetic efficiency for each block.

$$\eta_{Ex} = \frac{Ex_{OUT}}{Ex_{IN}} \quad (12)$$

3. Results and Discussion

3.1. Model Validation

In order to study the data extracted from the simulation, the model had to accurately reproduce how the plant performed in reality. To validate and check how accurate was the model developed using Aspen HYSYS®, the results were compared with the simplified process diagram of the industrial plant. In this respect, the model simulation was developed with the conditions shown in Section 2.1 above. Reformer and shift product compositions were compared to those obtained in the model, and the relative error was calculated as being the difference between the product composition at the real industrial plant and the data obtained from the simulator. Table 5 shows the error for the reformer and shift sections.

Table 5. Validation of the reformer and shift sections.

Compound	PFD Composition (mol % [db])	Model Composition (mol % [db])	Error (%)	PFD Composition (mol % [db])	Model Composition (mol % [db])	Error (%)
CH_4	7.4	7.5	2.4	6.5	6.2	4.1
CO	17.6	17.0	3.7	4.3	4.5	4.5
H_2	68.3	68.4	0.06	71.9	72.2	0.4
N_2	1.7	1.8	1.1	1.5	1.6	1.9
CO_2	4.7	5.1	8.8	15.5	15.2	1.7

[db]: dry base.

The model shown herein has been considered reliable because of the low relative errors found in the composition of the reformer and shift products, which were under 8.8% and 4.5% in the reformer and shift sections, respectively. Finally, in conclusion, the model was robust enough to study the performance of the industrial process.

3.2. Sensitivity Analysis

Once the model was validated, the influence of key variables was analysed with a sensitivity analysis with which the optimal operative conditions could be found. Thus, the response of different key variables in the process were studied when the operational parameters were modified. Two process variables were considered when studying the performance of the process: the molar ratio between raw

materials (steam-to-carbon molar ratio, S/C) and the reformer outlet temperature (T_{cc}). With this kind of analysis, it is possible to understand the energetic performance of the plant for a given variation interval for the previous studied variables. Several authors considered different variation intervals for these typical steam methane-reforming variables (T_{cc} = 760–980 °C and S/C = 1–2 [17]; T_{cc} = 0–1000 °C and S/C = 0–4 [5]). In this paper, the intervals for these process variables were selected by taking into account these studies as well as the historical process data from the industrial plant. Thus, the S/C interval was established between 0.5 and 4 and the T_{cc} varied between 750 and 1100 °C. In addition, the following parameters were studied: (1) heat flow of the reformer (heat flow), (2) hydrogen yield (the amount of hydrogen produced per mol of methane), (3) temperature difference in the shift reactor (ΔT_{Shift}) because energy is produced during the water-gas shift reaction (so the temperature in the reactor should increase if carbon monoxide is converted into carbon dioxide), and (4) hydrogen molar percentage at the reformer outlet ($H_{2\ ref\text{-}out}$).

The results are shown in Figures 2–4. It can be observed in Figure 2a that the energy demands of the reforming reaction increase with the S/C ratio. If the S/C ratio is increased, the amount of feed gas reacted in the reformer increases. As the SMR reaction is an endothermic reaction, the amount of energy necessary to carry out this reaction increases with the S/C ratio. In addition, if the amount of steam introduced in the furnace is increased for a given amount of feed, this steam also consumes energy when it is heated. When operating at a temperature over 900 °C and an S/C molar ratio over 2.5, the curve remained quite flat, which means that no more energy is consumed in the SMR reaction. This suggests that chemical equilibrium is reached if we use these operation conditions. However, operating at this temperature with this given S/C molar ratio could involve high energetic consumption. The energy needed for developing the reforming reaction also increased with T_{cc}, but the hydrogen yield when operating with a high S/C ratio and T_{cc} increased as well, as shown in Figure 2b. We noticed the same effect in this case: operating with high S/C molar ratio allows to reach a higher amount of hydrogen than with a low S/C molar ratio.

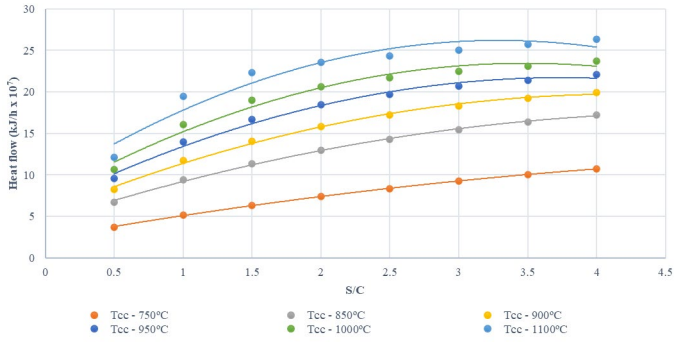

(**a**)

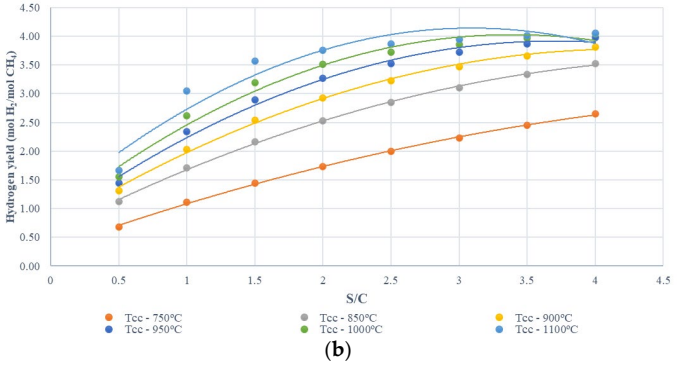

(**b**)

Figure 2. Comparison of different steam-to-carbon (S/C) molar ratios at different temperatures (T_{cc}) for (**a**) heat requirements (kJ/h) and (**b**) hydrogen yield (mol H_2/mol CH_4) at the REF block.

In order to find the best operative condition regions, a surface map has been plotted (Figure 3). The effect of ΔT_{Shift} and % of H_2 for T_{cc} and S/C molar ratio are shown in Figure 3a,b, respectively.

The evolution of ΔT_{Shift} (Figure 3a) shows that the optimal value of S/C for carrying out the shift reaction was found between 1.5 and 2.5. The ΔT_{Shift} decreased with S/C values over 2.5. This fact indicates that too high S/C ratios do not improve the water gas shift reaction. The higher the temperature in the reforming reaction, the higher the amount of CO generated, so the shift reaction improved significantly. However, this causes energetic consumption in the reformer to be too high.

In Figure 3b, the performance of the reforming reaction is shown. In this case, S/C and T_{cc} had a direct effect on hydrogen production. The amount of hydrogen produced in the reforming reactor increased with S/C and T_{cc}. However, values seemed to peak at 850 °C. Temperature became ever less influential over 900 °C, and the surface of the map became flat. Regarding the S/C molar ratio, this had to be at least 1.5. Above this value, the amount of hydrogen significantly increased. This means that, when a flat surface is achieved, any other increase in S/C molar ratio or in T_{cc} does not imply a significant increase in hydrogen production. If these plant conditions are achieved, the SMR would be operating at chemical equilibrium, so the maximum amount of hydrogen is obtained.

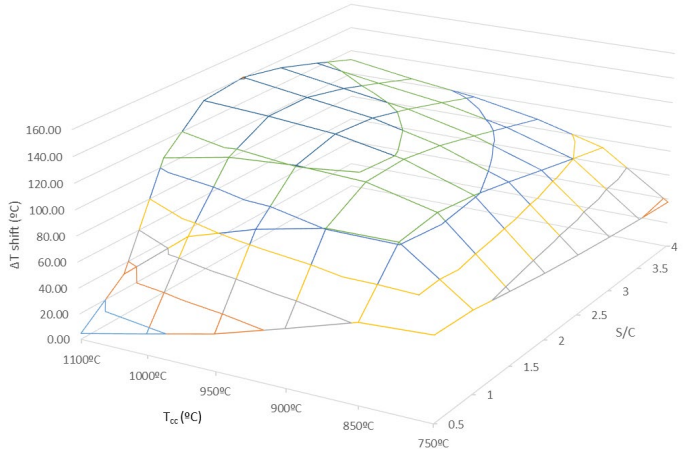

(**a**)

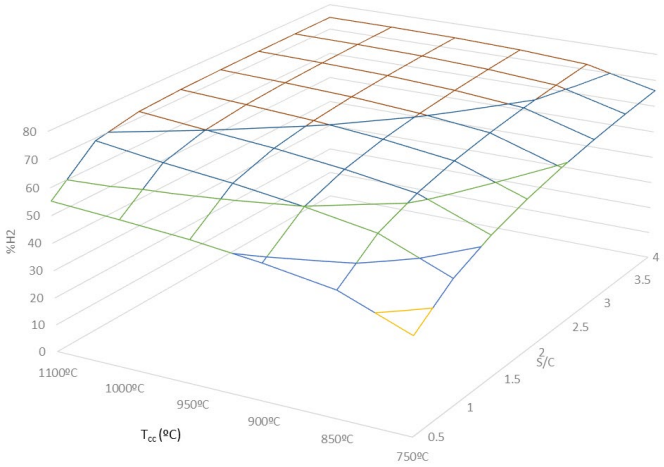

(**b**)

Figure 3. (**a**) Evolution of ΔT_{shift} (°C) for T_{cc} and S/C molar ratio and (**b**) profile of % H_2 for T_{cc} values and S/C molar ratio.

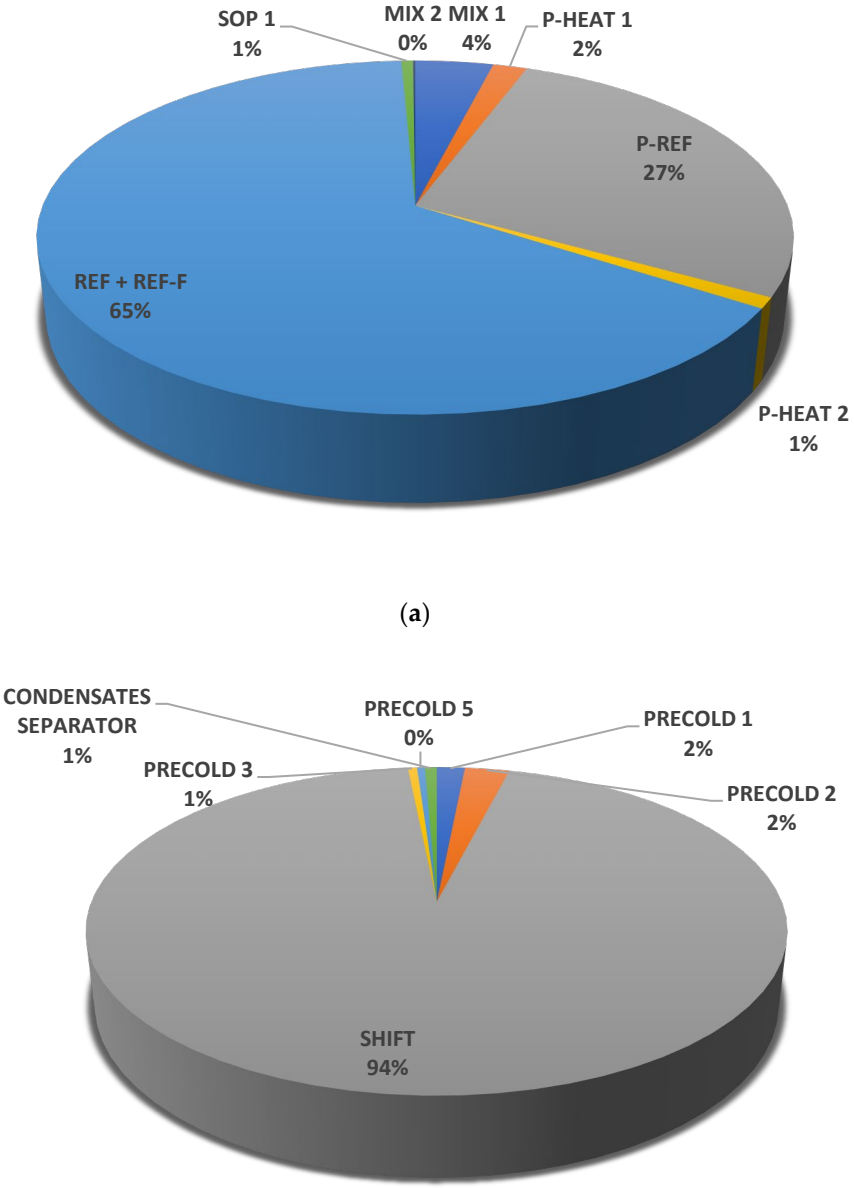

Figure 4. (**a**) Breakdown of unused exergy in Section 1; (**b**) breakdown of unused exergy in Section 2.

The optimum values for S/C ratio and T_{cc} were found to be 1.9 and 905 °C, respectively. In Table 6, the results obtained from the simulation are shown for each variable studied.

Table 6. Selected conditions after sensitivity analysis.

S/C = 1.9, T_{cc} = 905 °C	
$H_{2\ \text{ref-out}}$ * (mol %)	68
H_2 Yield (mol H_2/ mol CH_4)	2.9
ΔT_{Shift} (T_{in} = 210 °C) (°C)	120.5
Heat flow (kJ/h) ($\times 10^7$)	15.8

* mol % of H_2 obtained after reforming reactions.

These results concurred well with the productive objectives of the industrial plant. The hydrogen obtained after reforming reactions ($H_{2\ ref\text{-}out}$) was high enough to improve the objectives of production. The hydrogen yield reached an appropriate value, with almost 3 moles of hydrogen obtained per mole of NG. With these conditions, chemical equilibrium is expected to be achieved without overconsuming energy in the reforming reaction. The shift reactor showed a great ΔT over the packed bed, as desired. The energy requirements of the furnace were lower than expected for the given T_{cc} and the S/C ratio. This laid the foundations for studying energy optimization at later stages.

3.3. Exergetic Analysis

In Section 2.2, the equations to be applied for studying exergy were described. Once the sensitivity analysis finished, the parameters S/C ratio and T_{cc} were set. Then, each block of the simulation was studied by using exergy balances with which the amount of exergy destroyed in each part of the process and the exergetic efficiency of each block could be calculated. Table 7 shows the exergy destroyed in both sections, whereas Figure 4a,b shows a breakdown of the unused exergy by component as a percentage of total unused exergy.

Table 7. Exergetic analysis of Section 1 and Section 2.

Section 1			Section 2		
BLOCK	**EXERGY DESTROYED (kJ/kg·mol)**	η_{Ex} **(%)**	**BLOCK**	**EXERGY DESTROYED (kJ/kg·mol)**	η_{Ex} **(%)**
MIX 1	4004	98.81	PRECOLD 1	1074	98.26
P-HEAT 1	1751	98.41	PRECOLD 2	1698	99.26
P-REF	27749	91.64	SHIFT	65,943	68.19
P-HEAT 2	991.64	99.03	PRECOLD 3	352	99.76
REF + REF-F	65,865	55.89	PRECOLD 5	298	99.66
SOP 1	602	99.05	CONDENSATES SEPARATOR	455	99.51
MIX 2	114	99.95	-	-	-

As shown in Table 7, the major consumption of exergy was made on the chemical reactors. The exergetic performance of the heat exchangers of the process is higher than 98% for each heat exchanger studied. The pre-reforming reactor shows the best efficiency among all chemical reactors. This is an adiabatic reactor in which all products obtained present high chemical exergy, so the exergetic destruction is not so high in this reactor.

As expected, the blocks where the most exergy was consumed were REF + REF-F and SHIFT, whereas the other blocks showed relatively high values for exergetic efficiency. The origin of these losses was similar to that obtained by other researchers [10]. Exergy losses in the reformer were due to the chemical reactions taking place in this block (REF + REF-F). The irreversibility of the combustion reaction and the great amount of heat needed for these reactions mainly explained such a great exergy loss [18].

Similar behaviour was seen in the shift reactor, where CO was transformed into CO_2, which requires a great deal of exergy, as the chemical exergy of CO_2 (19,900 kJ/kmol) is quite lower than that for CO (275,100 kJ/kmol).

3.4. Exergetic and Economic Improvement

In order to improve the exergetic efficiency in the process as a whole, the unit where the most exergy was destroyed, the reformer reactor (REF + REF-F), was studied. There are many ways to improve exergetic performance that have been reported previously in the literature [2,14,19]. However, it must be stressed that only the options that were technically feasible and easy to implement at the plant were considered and that any possible modifications had to increase the profitability of the plant. For instance, adding a gas turbine is one typical solution for improving exergetic efficiency. However, this is not technically possible at the plant as the fall in pressure is not enough to produce a significant

amount of electric energy. Another possible solution is adding a bottoming cycle to recover part of the exergy, but this would entail technically unviable changes at the plant.

One interesting alternative for minimizing exergy losses that would not require significant modifications is optimizing the air stream flow fed to the unit REF-F. As explained in the work by Simpson et al. [7], there is a balance between the amount of air fed to the P-REF unit and the exergy destroyed. If this is high, the temperature of the combustion gases decreases, which leads to a decrease in the exergy destroyed in the reforming process. However, it also causes greater losses in exergy in the combustor and decreases the available energy in the flue gas stream. Therefore, an optimal value should be reached for the molar ratio between the air (represented as AIR stream in Figure 1a) and fuel (represented as TOTAL FUEL). Consequently, the optimal air/fuel ratio was calculated, and it varied from 4.2 to 8. Also, the exergetic efficiency of P-HEAT 1, P-HEAT 2 and REF + REF-F units was recalculated and compared with the optimal value found previously. The results are shown in Figure 5. As expected, a maximum value for exergetic efficiency in the reformer reactor (REF + REF-F) was found, which peaked with an air/fuel molar ratio of 6. This value showed an increase in exergetic efficiency of up to 63%. An excessively high amount of air in the reformer furnace provokes more exergetic losses because a high amount of heat is removed from the furnace within the fumes. On the other hand, if the amount of air introduced in the furnace is too low, the energy obtained from combustion would be low as well. This process modification is not associated with an economical investment; however, the flue gas fan could be limited if the air requirements of the furnace are too high. In this case, the exergetic efficiency obtained is high if we compare it with other similar processes.

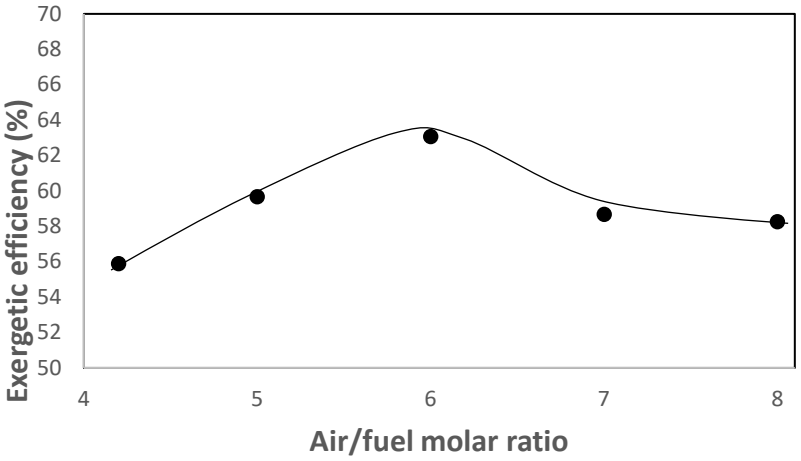

Figure 5. Evolution of exergetic efficiency vs. air/fuel molar ratio.

In order to evaluate the economic impact of the variation of the air/fuel molar ratio at the industrial plant, a preliminary economic study was carried out (Table S3). Savings in energy cost of 22% per year were observed with an air/fuel molar ratio of 6. Thus, exergy of at the industrial plant could be improved without any additional cost, and so, implementing this was feasible.

4. Conclusions

An Aspen HYSYS® simulation of the steam methane-reforming process based on data from an industrial plant was carried out successfully. Having validated the simulation, there was a sensitive analysis in order to study the most important variables in the industrial process. In addition, an exergetic analysis was conducted to locate exergy losses in steam reforming. Several conclusions were reached, which are as follows:

(1) The simulation was robust enough to reproduce the behaviour at the industrial plant. The results have been quite similar to those actually found at steam methane-reforming plants.

(2) The sensitive analysis enabled us to identify optimal values for the steam-to-carbon molar ratio and the reformer outlet temperature (1.9 and 905 °C, respectively).
(3) With the exergetic analysis, we could find exact exergy losses in the different sections of the industrial process. The highest amount of exergy was destroyed in the chemical reactors, and it was lost on account of the thermodynamic irreversibility of these chemical reactions.
(4) The exergetic efficiency of the reforming reactor could be improved by modifying the molar ratio between the air and fuel fed to the combustor (REF-F). With an air/fuel molar ratio of 6, the exergetic efficiency in the REF + REF-F increased from 56% to 63%.
(5) The economic assessment of the influence of the air/fuel molar ratio showed that consumption of electricity and natural gas fell by up to 22%, with a+ air/fuel molar ratio of 6. Therefore, this improvement saved not only energy but also money.
(6) This analysis is useful for a given value of total hydrogen flow. However, it is limited because it does not consider variations in hydrogen production.
(7) In this analysis, reactor kinetic equations are not considered. The results obtained from the simulation could be more robust if kinetic equations were implemented in the process reactors (P-REF + REF + SHIFT).
(8) The steam generation unit should be considered in further analysis. The exergetic performance of the furnace would improve because all the heat in flue gas would have been recovered.

Supplementary Materials: The following are available online at http://www.mdpi.com/1996-1073/13/15/3807/s1, Table S1: Natural gas composition, Table S2: SYN-GAS HDS composition, Table S3. Utility costs for air/fuel molar ratio of 6.

Author Contributions: Conceptualization, F.D. and L.S.-S.; Methodology, L.S.-S.; Software, F.J.D.; Validation, F.J.D.; Formal Analysis, F.D.; Investigation, F.J.D.; Writing-Original Draft Preparation, F.J.D.; Writing-Review & Editing, F.D. and L.S.-S.; Supervision, F.D. and L.S.-S. All authors have read and agreed to the published version of the manuscript.

Funding: This research received no external funding.

Acknowledgments: In this section you can acknowledge any support given which is not covered by the author contribution or funding sections. This may include administrative and technical support, or donations in kind (e.g., materials used for experiments).

Conflicts of Interest: The authors declare no conflict of interest.

References

1. Da Silva Veras, T.; Mozer, T.S.; da Costa Rubim Messeder dos Santos, D.; da Silva César, A. Hydrogen: Trends, production and characterization of the main process worldwide. *Int. J. Hydrogen Energy* **2017**, *42*, 2018–2033. [CrossRef]
2. Dincer, I.; Acar, C. Smart energy solutions with hydrogen options. *Int. J. Hydrogen Energy* **2018**, *43*, 8579–8599. [CrossRef]
3. Nikolaidis, P.; Poullikkas, A. A comparative overview of hydrogen production processes. *Renew. Sustain. Energy Rev.* **2017**, *67*, 597–611. [CrossRef]
4. Abbas, S.Z.; Dupont, V.; Mahmud, T. Kinetics study and modelling of steam methane reforming process over a NiO/Al2O3 catalyst in an adiabatic packed bed reactor. *Int. J. Hydrogen Energy* **2017**, *42*, 2889–2903. [CrossRef]
5. Imran, U.; Ahmad, A.; Othman, M. Kinetic Based Simulation of Methane Steam Reforming and Water Gas Shift for Hydrogen Production Using Aspen Plus. *Chem. Eng. Trans.* **2017**, *56*, 1681–1686.
6. Pashchenko, D. First law energy analysis of thermochemical waste-heat recuperation by steam methane reforming. *Energy* **2018**, *143*, 478–487. [CrossRef]
7. Cui, X.; Kær, S.K. Thermodynamic analysis of steam reforming and oxidative steam reforming of propane and butane for hydrogen production. *Int. J. Hydrogen Energy* **2018**, *43*, 13009–13021. [CrossRef]
8. BoroumandJazi, G.; Rismanchi, B.; Saidur, R. A review on exergy analysis of industrial sector. *Renew. Sustain. Energy Rev.* **2013**, *27*, 198–203. [CrossRef]

9. Kaini, B.; Mondal, K. Thermodynamic evaluation of hydrogen production from methane. *Int. J. Hydrogen Energy* **2014**, *39*, 17671–17689. [CrossRef]
10. Díez-Ramírez, J.; Dorado, F.; Martínez-Valiente, A.; García-Vargas, J.M.; Sánchez, P. Kinetic, energetic and exergetic approach to the methane tri-reforming process. *Int. J. Hydrogen Energy* **2016**, *41*, 19339–19348. [CrossRef]
11. Cruz, P.L.; Navas-Anguita, Z.; Iribarren, D.; Dufour, J. Exergy analysis of hydrogen production via biogas dry reforming. *Int. J. Hydrogen Energy* **2018**, *43*, 11688–11695. [CrossRef]
12. Behroozsarand, A.; Wood, D.A. Comparison of Exergy Losses for Reformers Involved in Hydrogen and Synthesis Gas Production. *Chem. Eng. Technol.* **2019**, *42*, 2681–2690. [CrossRef]
13. Khila, Z.; Baccar, I.; Jemel, I.; Houas, A.; Hajjaji, N. Energetic, exergetic and environmental life cycle assessment analyses as tools for optimization of hydrogen production by autothermal reforming of bioethanol. *Int. J. Hydrogen Energy* **2016**, *41*, 17723–17739. [CrossRef]
14. Tzanetis, K.F.; Martavaltzi, C.S.; Lemonidou, A.A. Comparative exergy analysis of sorption enhanced and conventional methane steam reforming. *Int. J. Hydrogen Energy* **2012**, *37*, 16308–16320. [CrossRef]
15. Quimitube. Termodinámica Teoría 10: Definición de Entalpía de Formación y Ejemplos. Available online: http://www.quimitube.com/videos/termodinamica-teoria-10-definicion-de-entalpia-de-formacion-y-ejemplos (accessed on 20 May 2018).
16. Segundo y Tercer Principio de la Termodinámica. 2018. Available online: iesdmjac.educa.aragon (accessed on 20 May 2018).
17. Giwa, A.; Giwa, S. Simulation, Sensitivity Analysis and Optimization of Hydrogen Production by Steam Reforming of Methane Using Aspen Plus. *Int. J. Eng. Res. Technol.* **2013**, *2*, 1719–1729.
18. Chen, B.; Liao, Z.; Wang, J.; Yu, H.; Yang, Y. Exergy analysis and CO_2 emission evaluation for steam methane reforming. *Int. J. Hydrogen Energy* **2012**, *37*, 3191–3200. [CrossRef]
19. Dincer, I.; Acar, C. Review and evaluation of hydrogen production methods for better sustainability. *Int. J. Hydrogen Energy* **2015**, *40*, 11094–11111. [CrossRef]